NANO LETTERS

2001
Vol. 1, No. 11
589−593

Shape Dependent Ultrafast Relaxation Dynamics of CdSe Nanocrystals: Nanorods vs Nanodots

Mona B. Mohamed, Clemens Burda,† and Mostafa A. El-Sayed*

Laser Dynamics Laboratory, School of Chemistry and Biochemistry, Georgia Institute of Technology, Atlanta, Georgia 30332-0400

Received July 17, 2001; *Revised Manuscript Received September 6, 2001*

ABSTRACT

Femtosecond pump–probe transient spectroscopy is used to compare the time dependence of the bleach recovery of CdSe nanorods with that of nanodots. In the quantum dots the bleach spectrum evolved rapidly to its characteristic shape, while in the nanorods, the higher energy exciton states are first populated within the laser pulse width (100 fs) and then relax to lower states. This behavior is explained by the larger number of exciton states in the rods due to splitting of the degeneracy of the states in the dots as a result of the decrease in symmetry as predicted from existing theories.

Semiconductor nanocrystals present us with an important system for the study of fundamental physics[1−4] as well as their potential applications in optoelectronic devices and nanotechnology.[5−7] The ultrafast optical and electronic responses of semiconductor nanocrystals are completely different from the bulk semiconductor materials due to quantum confinement effect.[1−4] In semiconductor quantum dots (QDs), the motion of the carriers is restricted in space, which changes the band gap energy and leads to discrete electronic levels with a quantized energy spacing. The energy spacing between these electronic energy levels and the band gap of the semiconductor nanodots depends on the size of the crystals.[3,4] The band gap increases by decreasing the average size of the semiconductor nanocrystals. Special interest is focused in studying semiconductor nanoparticles because of the fact that their optical and electric properties can be tuned simply by changing their size or their surface characterizatics.[8−12]

Significant progress has been made in understanding the energy relaxation and recombination dynamics in semiconductor nanodots (NDs) such as CdS,[13] CdS/HgS/CdS QDQW,[14−19] and CdSe[20−27] nanoparticles. These previous studies were focused on studying the relaxation dynamics dependence on the size of the crystals, their surface properties, and the chemical composition. No studies have yet been reported on the dependence of the relaxation processes on shape. This is the focus of this communication.

The most interesting recent development in semiconductor nanoscience is the ability to synthesize semiconductor nanocrystals where shape control[28−30] and doping[31] can be achieved. This allows us to study experimentally how the optical properties of semiconductor nanoparticles depend on shape. Recently, Alivisatos' group[28,29] were able to obtain CdSe nanorods (NRs) of different aspect ratios by the injection of a mixture of Cd $(CH_3)_2$ and Se metal dissolved in trioctlphosphine (TOP) into a binary mixture of surfactant such as trioctylphosphine oxide (TOPO) and hexylphosphonic acid (HPA) at 300 °C. They found that the aspect ratio of CdSe NRs depends on the ratio between the two surfactants. In addition, they studied the absorption and emission properties and they reported that the band gap of CdSe NRs depends mainly on the width and slightly on the length.[32] They also studied the emission properties of these CdSe NRs using single-molecule luminescence spectroscopy. They found that the CdSe NRs exhibit linearly polarized emission along their long axis.[33]

In this Letter, we report the time dependence of the femtosecond transient bleach spectrum of CdSe NRs compared to that of the nanodots (NDs). Our results show that the electron−hole relaxation dynamics is quite different in nanorods of aspect ratio ∼3 than those of the nanodots of 4.2 nm diameter. These results are discussed in terms of splitting of the degeneracy of the energy levels of the nanodots due to lowering of their symmetry. This is supported by the rich bleach spectrum observed for the NRs as compared with that for the NDs.

CdSe NDs are prepared according to the procedure developed by Murray et al.,[34] with minor modification. A

* Corresponding author. E-mail: mostafa.el-sayed@chemistry.gatech.edu.
† Current address: Chemistry Department, Case Weston Reserve University, Cleveland, OH 44106.

10.1021/nl0155835 CCC: $20.00
Published on Web 10/12/2001

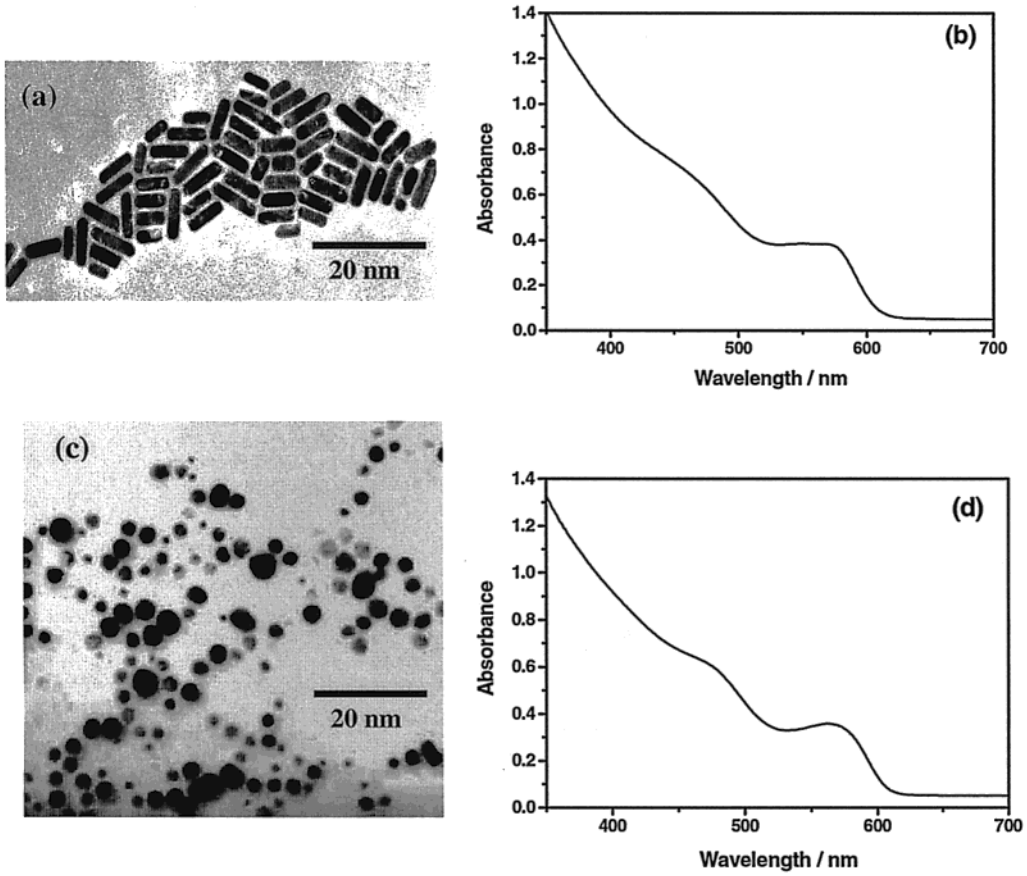

Figure 1. TEM image of spotted CdSe nanorods (a) and the absorption spectrum of its solution (b). (c) TEM image of the spotted CdSe nanodots whose solution absorption spectrum is given in (d).

0.5 mL aliquot of Cd $(CH_3)_2$ is added to 3 mL of trioctylphosphine (TOP) in a vessel. In another vessel 0.2 g of Se powder is dissolved in 5 mL of TOP. The contents of the two vessels are mixed together under Ar atmosphere and injected rapidly into a hot solution of trioctylphosphine oxide (TOPO) (300 °C). To prepare CdSe NRs using the same approach, which was developed recently,[28−30] the mixture of $Cd(CH_3)_2$ and Se in TOP is injected rapidly into a hot solution of a mixture of binary surfactant composed of TOPO + hexylphosphonic acid (HPA) (2:1 ratio at 300 °C). The CdSe nanoparticles were isolated from the reaction mixture by adding ~50 mL of methanol (to cool the reaction and stop further growth of the particles), followed by centrifugation. Repeated washing of the isolated particles with methanol was necessary to remove the excess TOPO. The CdSe nanoparticles are obtained as a powder, which is highly soluble in toluene or hexane.

The freshly prepared sample of CdSe nanorods (NRs) was analyzed by a Hitachi HF-2000 field emission transmission electron microscope operating at 200 kV. Counting over 300 particles resulted in an average width of 4.2 ± 0.6 nm and an average length of 13.5 ± 1.5 nm, giving an average aspect ratio of ~3. The contamination of the sample by spherical or quasispherical CdSe nanoparticles is estimated to be less than 10%. The average diameter of CdSe nanodots is found to be 4.2 ± 1.0 nm. TEM images of the CdSe NRs and NDs are shown in Figure 1.

The relaxation dynamics of the CdSe nanocrystals are studied using an amplified Ti−Sapphire femtosecond laser system (Clark MXR CPA 1000) pumped by a frequency-doubled Nd:vanadate laser (Coherent Verdi). This produces laser pulses of 100 fs duration (HWFM) with energy of 1 mJ at 800 nm. The repetition rate was 1 kHz. A small portion of the fundamental pulses (about 40 μJ) was used to generate a femtosecond white light continuum in a 1 mm sapphire plate. The range of the femtosecond continuum is between 450 and 1000 nm and is used as a probe beam. The probe beam was split into two beams, a signal and a reference beam. The second harmonic from the Ti:sapphire laser (400 nm) was used as the pump beam. This excitation beam passes through a computer-controlled optical delay line with a resolution of 3 μm (22 fs). The pump and the signal beams were overlapped into the sample. The signal and reference beams were focused into fiber optics coupled to a monochromator. The excitation beam was modulated by an optical chopper at a frequency of 500 Hz with the same phase. Two photodiodes were employed for the kinetic measurements at the exit slit of the monochromator. The photocurrent from the signal and reference photodiodes was amplified and passed through a sample and hold circuitry and coupled to a lock-in amplifier locked at 500 Hz. The delay line was repeatedly scanned until a reasonable signal-to-noise ratio was achieved. The typical optical density (OD) changes measured were in the range 5−200 mOD. For spectral

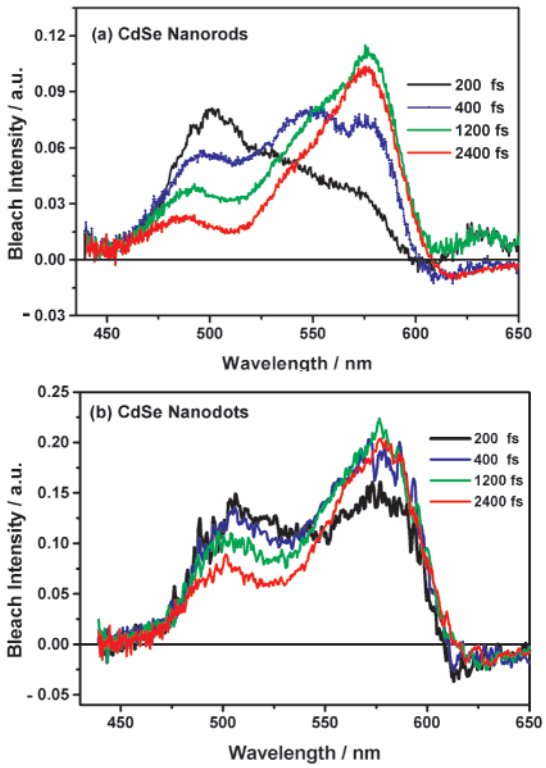

Figure 2. Shape dependent ultrafast electron−hole relaxation in CdSe nanocrystals in early time 200 fs to 2.4 ps at the spectral range 440−650 nm. The change in dynamics over the same spectral range is less pronounced for nanodots than for nanorods.

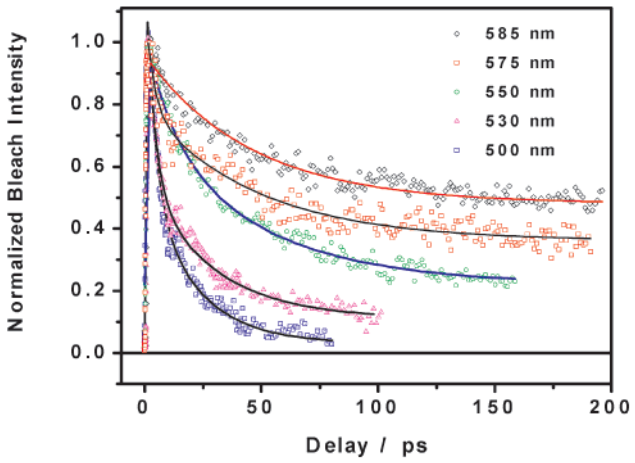

Figure 3. Decay kinetics of CdSe nanorods at different probe wavelengths showing that the relaxation is faster for the higher energy states (see Table 1).

Table 1. Comparison between the Exciton Relaxation Dynamics of the Different States in CdSe Nanorods and CdSe Nanodots[a]

probe wavelength (nm)	CdSe nandorods			CdSe nanodots		
	decay times		rise times	decay times		rise times
	T_1	t_2, ps		t_1, ps	t_2, ps	times, fs
585	50.0 ps		∼1.0 ps	2.05	36.1	∼400
575	3.5 ps	47.0	∼750 fs			
550	4.3 ps	43.0	∼540 fs	2.2	33.0	∼350
530	4.1 ps	20.0	∼470 fs			
515	330 fs	3.7	<100 fs	2.25	28.0	<100
500	350 fs	3.1	<100 fs			
480	300 fs	2.1	<100 fs	2.6	21.9	<100

[a] The excitation Wavelength is 400 nm. The laser pulse width is 100 fs.

measurements a charge coupled device (CCD) camera (Princeton Instruments) attached to a spectrograph (Acton Research) was used. The CdSe sample solution was placed in a 2 mm cylindrical glass cuvette. All experiments were performed at room temperature.

Figure 2 compares the change in the bleach spectrum of the nanorods (Figure 2a) with that of the nanodots (Figure 2b) using the same delay times of 200 fs, 400 fs, 1.2 ps, and 2.4 ps in each spectrum. In both spectra, the same laser pump wavelength and energy were used. The continuum white light, which was used as a probe beam, does not have much intensity below 450 nm. Thus, the spectrum could not be recorded between 400 and 450 nm. Within 200 fs, the carriers seem to distribute themselves among fewer energy states in the dots compared to the rods. This allows the $1S_e - 1S_{h(3/2)}$ (band gap state at 585 nm) to have a higher population than the corresponding state in the quantum rods. As the delay time increases, the spectrum of the dot does not change much, while in the NRs, the population of the higher excitonic states relaxes rapidly to the lower states and finally to the band gap state. (Compare the changes in the spectrum in black color with that in red in each spectrum given in Figure 2a,b.)

Femtosecond time-resolved pump−probe spectroscopy allows the determination of the rise and decay time of the population density of the different energy levels. We have excited both samples with low power excitation (1 μJ) at 400 nm to avoid biexciton formation and Auger processes. We monitored the bleach lifetime at several wavelengths between 460 and 600 nm (see Figure 3 and Table 1). Figure 3 shows that the decay is faster for the higher energy exciton states.

In Figure 4, the band gap bleach kinetics of the CdSe nanorods (blue squares) and nanodots (red circles) are compared. It is observed that both the rise and decay times are longer for the rods compared to those for the dots. Table 1 shows a summary of the kinetic results of the rise and the bleach decay monitored for the different peaks appearing in the spectra for both the NRs and NDs.

The conclusions that can be drawn from the results shown in Figures 3 and 4 and Table 1 follow: (1) The rise time of the high-energy states (at 480 nm) is very fast in both particles (within the laser pulse width which is 100 fs. (2) The rise time of the band gap state is faster in the dots (400 fs) as compared to the rods (∼1.0 ps). (3) The decay of the higher energy state is much faster in the rods as compared to the dots (300 fs vs 2 ps). (4) For the rods, the decay becomes longer as the energy decreases (300 fs for states in the 480−515 nm range, a few picoseconds for states in the 530−575 nm range, and 50 ps at the band gap state). (5) The decay time of the band gap state (at 585 nm) is longer for the rods (50 ps) compared to that for the dots (2.0 or 36

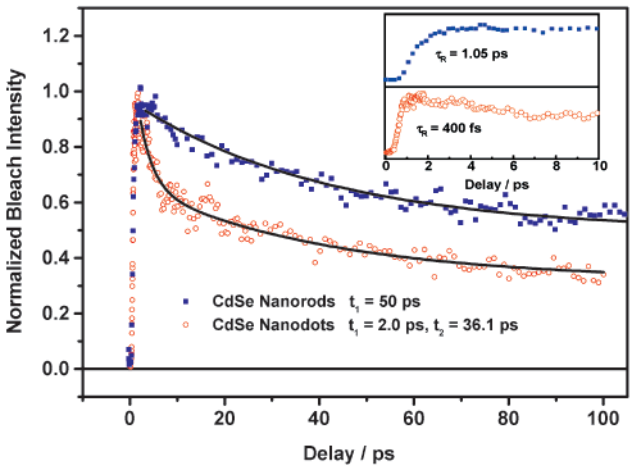

Figure 4. Comparison between the rise and the decay kinetics of the CdSe nanorods and nanodots at 585 nm wavelength (at the band gap) showing that the rise and decay in the case of nanorods is much slower than that of the dots.

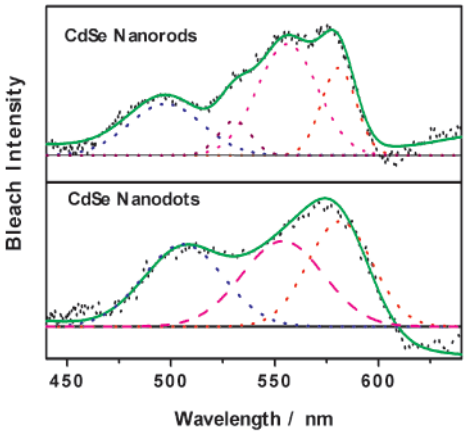

Figure 5. Deconvolution of the early time bleach spectra of CdSe nanorods and nanodots.

ps). This might be due to less effective surface trapping in the rods.

The above kinetic results are consistent with the time dependence of the observed bleach spectra in Figure 2. Within the pulse width (100 fs), a good fraction of the population seems to occupy the lower energy levels present in the dots as well as the high energy levels of the rods. As the delay time increase, no large change in the spectrum of the dots takes place, while in the rods, the cascade between the many levels slows down the spectral development of the bleach spectrum of the band gap state at 585 nm.

These dynamics data could be understood if the predicted splitting[35−41] of the energy levels upon elongation of the dots into rods is taken into account. Simple calculations, based on the effective mass approximation,[42,43] have been preformed to study the quantum confinement of semiconductor nanocrystals whose shape is different from the usual spherical shape.[35−41] Cantele et al.[38,39] calculated the confined state and the infrared optical transitions in semiconductor ellipsoidal quantum dots. Their study shows that the confined state energies split with respect to those of the spherical quantum dot. They attributed these results to a consequence of the volume-induced deformation effect and also the geometry-induced one. Decreasing the degree of symmetry and the anisotropy effect lead to changing of the degeneracy and splitting of the excited states of semiconductor nanostructures of cylindrical or ellipsoidal shapes. This depends mainly on the actual shape geometry of the crystal. Moreover, the authors found that the dot geometry also plays an important role in the formation of topological surface states. Because of the fact that the carriers are confined in the neighborhood of the nanocrystal surface, states localized along the surface can arise. The localization of these surface states is induced by the surface curvature. If the particle has ellipsoidal or cylindrical shape, one axis is longer than the other. Along the long axis the carrier motion is free, whereas on an undulating surface, the carrier may be trapped. The surface states are dependent strongly on the surface curvature variations. This might introduce different surface states in the ellipsoidal or cylindrical shape quantum dots than that in the spherical dots.

Using simple variational calculation for a model of a microcrystal with cylindrical shape, the shape dependence of the quantum size effect has been studied.[39,40] A more recent study has been performed using an empirical pseudopotential calculation to calculate the electronic structure of surface-passivated CdSe quantum dots.[44] Using the same approach, the electronic structure of the CdSe nanocrystal has been calculated[33] as the shape evolves from spherical to rodlike particle by inserting a cylindrical segment along the *c* axis. They calculated the four lowest unoccupied and the four highest occupied electronic states for quantum rods with aspect ratio ranging from 1.0 to 5.0. They found that the $4P_z$ orbital has greater momentum projected onto the *c* axis of the crystal. This led to splitting of the 4P orbital into $4P_x$-$4P_y$ and $4P_z$ and the $4P_z$ energy level is more sensitive to the rod length.

The fast carrier relaxation dynamics of the higher energy states in the rods compared to that in the dots could be explained by the fact that lowering the symmetry in the rods leads to splitting of the degeneracy of the energy levels in the dots. It should be mentioned that the increase in the density of states leads to an increase in the relaxation process involving either electron−phonon or electron−hole coupling.[22] The smaller the electron energy separation, the more likely phonons or holes can be found to accept the released energy and thus the faster the relaxation would be.

The deconvolution of the bleach spectra at early time (1 ps) is shown for both the dots and the rods in Figure 5. In agreement with the size distribution results in Figure 1a,c, the bands of the dots are much broader than those of the rods (which have very narrow size distributions). Despite this large inhomogeneous broadening observed in the bleach spectrum of the dots, their deconvoluted spectrum shows three bands with energies in agreement with those reported in the literature.[22,26] From Figure 5, it is clear that the rods have more absorption bands than the dots due to the splitting of the corresponding degenerate states in the dots.

Acknowledgment. This work was supported by the Office of Naval Research, Grant No. N00014-95-1-0306). M.M thanks the Egyptian Government Mission Department for a Ph.D. scholarship. We thank M. Braun for providing the chirp-correction program.

References

(1) Steigerwald, M. L.; Brus, L. E. *Acc. Chem. Res.* **1990**, *23*, 183. Brus, L. E. *J. Chem. Phys.* **1983**, *79*, 5566. Brus, L. E. *J. Chem. Phys.* **1984**, *80*, 4403. Brus, L. *IEEE J. Quantum Electron.* **1986**, *QE−22* (9), 1909.
(2) Wang, Y.; Herron, N. *J. Phys. Chem.* **1991**, *95*, 525.
(3) Haase, M.; Weller, H.; Henglein, A. *J. Phys. Chem.* **1988**, *92*, 4706.
(4) Chestnoy, N.; Harris, T. D.; Hull, R.; Brus, L. E. *J. Phys. Chem.* **1986**, *90*, 3393.
(5) Alivisatos, A. P.; Harris, A. L.; Levinos, N. J.; Steigerwald, M. L.; Brus, L. E. *J. Chem. Phys.* **1988**, *89* (7), 4001−4011.
(6) Heath, J. R. *Science* **1995**, *270* (5240), 1315−1316.
(7) Alivisatos, A. P. *J. Phys. Chem.* **1996**, *100* (31), 13226.
(8) Nirmal, M.; Dabbousi, B. O.; Bawendi, M. G.; Macklin, J. J.; Trautman, J. K.; Harris, T. D.; Brus, L. E. *Nature* **1996**, *383* (6603), 802−804.
(9) Heath, J. R.; Williams, R. S.; Shiang, J. J.; Wind, S. J.; Chu, J.; Demic, C.; Chen, W.; Stanis, C. L.; Bucchignano, J. J. *J. Phys. Chem.* **1996**, *100* (8), 3144−3149.
(10) Zhang, J. Z. *Acc. Chem. Res.* **1997**, *30* (10), 423−429.
(11) Brus, L. *Appl. Phys. A: Solids Surf.* **1991**, *53* (6), 465−474.
(12) Wang, Y. *Acc. Chem. Res.* **1991**, *24* (5), 133−139.
(13) Logunov, S. L.; Green, T.; Marguet, S.; El-Sayed, M. A. *J. Phys. Chem. A* **1998**, *102* (28), 5652.
(14) Mews, A.; Kadavanich, A.; Banin, U.; Alivisatos, A. P. *Phys. Rev. B* **1996**, *53*, 13242.
(15) Kamalov, Valey F.; Little, Reginald; Logunov, Stephan L.; El-Sayed, Mostafa A. *J. Phys. Chem.* **1996**, *100* (16), 6381.
(16) Little, R. B.; Burda, C.; Link, S.; Logunov, S.; El-Sayed, M. A. *J. Phys. Chem. A* **1998**, *102*, 6581.
(17) Braun, M.; Burda, C.; Mohamed, M. B.; El-Sayed, M. A. *Phys. Rev B* **2001**, *64*, 035317.
(18) Braun, M.; Burda, C.; El-Sayed, M. A. *J. Phys. Chem. A* **2001**, *105*, 5548.
(19) Little, Reginald, B.; El-Sayed, Mostafa, A.; Bryant, Garnett, W.; Burke, Susan *J. Chem. Phys.* **2001**, *114* (4), 1813.
(20) Burda, C.; Green, T. C.; Link, S.; El-Sayed, M. A. *J. Phys. Chem. B* **1999**, *103* (11), 1783−1788.
(21) Hines, M A.; Guyot-Sionnest, P. *J. Phys. Chem. B* **1998**, *102* (19), 3655.
(22) Klimov, V. I. *J. Phys. Chem. B* **2000**, *104* (26), 6112.
(23) Underwood, D. F.; Kippeny, T.; Rosenthal, S. J. *J. Phys. Chem. B* **2000**, *104* (7), 1494.
(24) Klimov, V. I.; Schwarz, Ch. J.; McBranch, D. W.; Leatherdale, C. A.; Bawendi, M. G. *Phys. Rev. B: Condens. Matter Phys.* **1999**, *60* (4), R2177.
(25) Klimov, V. I.; McBranch, D. W. *Phys. Rev. Lett.* **1998**, *80* (18), 4028.
(26) Klimov, V. I.; Mikhailovsky, A. A.; McBranch, D. W.; Leatherdale, C. A.; Bawendi, M. G. *Phys. Rev. B: Condens. Matter Phys.* **2000**, *61* (20), R13349.
(27) Klimov, V. I. In Optical Properties. *Handbook of Nanostructured Materials and Nanotechnology*; Nalwa, H. S., Ed.; Academic Press: New York, 2000; Vol. 4.
(28) Xiaogang, P.; Manna, L.; Yang, Weidong; Wickham, J.; Scher, E.; Kadavanich, A.; Alivisatos, A. P. *Nature* **2000**, *407*, 981.
(29) Manna, L.; Scher, Erik, C.; Alivisatos, A. P. *J. Am. Chem. Soc.* **2000**, *122*, 12700.
(30) Peng, Adam, Z.; Xiaogang, P. A. *J. Am. Chem. Soc.* **2000**, *123*, 1389.
(31) Shim, M.; Guyot-Sionnest, P. *Nature* **2000**, *407*, 981.
(32) Li, Liang-Shi; Hu, J.; Yang, W.; Alivisatos, A. P. *Nano Lett.* **2001**, *1* (7), 349.
(33) Hu, J.; Li, L.; Yang, W.; Manna, L.; Wang, Lin-Wang; Alivisatos, A. P. *Science* **2001**, *292*, 2060.
(34) Murray, C. B.; Norris, D. J.; Bawendi, M. G. *J. Am. Chem. Soc.* **1993**, *115*, 8706.
(35) Efros, A. L.; Arondina, A. V. *Phys. Rev. B* **1993**, *47*, 10005.
(36) Ninno, D.; Iadonisi, G.; Buonocore, F. *Solid State Commun.* **1999**, *112*, 521.
(37) Buonocore, F.; Ninno, D.; Iadonisi, G. *J. Phys., Condens. Matter* **2000**, *112*, 521.
(38) Cantele, G.; Ninno, D.; Iadonisi, G. *J. Phys., Condens. Matter* **2000**, *12*, 9019.
(39) Cantele, G.; Ninno, D.; Iadonisi, G. *Nano Lett.* **2001**, *1* (3), 121.
(40) Kayanuma, Y. *Phys. Rev. B* **1991**, *44*, 13085.
(41) Goff, S. Le.; Stébé, B. *Phys. Rev. B* **1993**, *47*, 1383.
(42) Brus, L. *J. Phys. Chem.* **1986**, *90*, 2555.
(43) Yoffe, A. D. *Adv. Phys.* **1993**, *42*, 173.
(44) Wang, Lin-Wang; Zunger, A. *Phys. Rev. B* **1996**, *53*, 9579.

NL0155835